ISO[1] Long Wavelength Spectrograph Observations of Cold Dust in Galaxies

Matthew Trewhella

IPAC (Caltech/JPL), 770 S. Wilson Ave., Pasadena, CA 91125, USA

and

Jonathon I. Davies, Paul B. Alton and Simone Bianchi

Dept. of Physics and Astronomy, University of Wales Cardiff,

The Parade, Cardiff CF2 3YB, UK

and

Barry F. Madore

NASA/IPAC Extragalactic Database (NED), 770 S. Wilson Ave., Pasadena, CA 91125, USA & Observatories of the Carnegie Institute of Washington, 813 Santa Barbara St., Pasadena, CA 91101, USA

Received ______________; accepted ______________

To appear in the Astrophysical Journal

---

[1]Based on observations with *ISO*, an ESA project with instruments funded by ESA Member States (especially the PI countries: France, Germany, the Netherlands and the United Kingdom) with the participation of ISAS and NASA.

ABSTRACT

We describe observations of 5 nearby galaxies obtained using the Long Wavelength Spectrograph (LWS) on the Infrared Space Observatory (ISO). We observed 5 galaxies, using spectrograph apertures positioned at the galactic center and in the outskirts of the disk, to compare the spectral energy distribution of the emitting dust at different positions. The central spectra are typical of those inferred previously from IRAS data; peaking at about 100 μm with estimated dust temperatures of $T_d = 30 - 35°$K. However, there is a rapid change in the spectral energy distribution with increasing galactocentric distance. In the outer regions the spectra are flat, or still rising, out to $197\mu m$ indicating a predominantly cold dust component with $T_d < 20°$ K. In the central regions, the inferred cold dust mass is approximately an order of magnitude larger than that associated with the warm dust and increasingly dominates the dust mass even more in the outer regions. We discuss reasons for believing that emission beyond $\approx 150\mu m$ in disk galaxies is associated with a seperate component of dust with an extended distribution that may be associated with a possible molecular halo.

Subject headings: dust, extinction - galaxies - general

1. Introduction

Some of the most important problems facing extragalactic astronomers today revolve around the interpretation of observations of a 'dusty' Universe. These include the relationship between the UV energy density and the star formation rate as a function of redshift; the strong evolution of infrared bright galaxies; and measurements of the far infrared cosmic background. An important tool to help us interpret the many observations that can be made of galaxies is found in radiative transfer models that are able to predict both the extinction by and the emission from dust (Kylafis and Bahcall 1987, Disney, Davies & Phillipps 1989, Witt, Thronson & Capuano 1992, Bianchi, Ferrara & Giovanardi 1996, Trewhella, Madore and Kuchinski 1999). The basic input to such models are the physical properties and relative distribution of the extinguishing material and the heating sources (i.e. for galaxies, the 3D spatial distribution of stars and dust). We have recently obtained observations, over a wide range of wavelengths, of nearby, large-angular-size galaxies to try to define more precisely the input parameters to these radiative transfer models.

A large source of uncertainty in, and a crucial component of, the models is the relative geometry of the stars and dust. For a point source seen through a screen of dust (as when viewing stars in our galaxy), the radiative transfer is relatively simple and many classic techniques (e.g. Hiltner & Johnson 1956) exist to correct stellar magnitudes for extinction. It has proved difficult however, to find such simple methods to correct the observed, global properties of galaxies for the obscuring effects of dust (Disney et al. 1989). As yet, no straightforward and unambiguous diagnostic for dust extinction exists for composite stellar systems, even though all areas of extragalactic astronomy that rely on measurement of luminosity and color are affected by it. It is likely that this will remain the case until we have a better understanding of the detailed dust distribution in galaxies.

A major open question has been how the cold dust, ($< 20K$) which could not be detected by the InfraRed Astronomical Satellite (IRAS), behaves. We will argue that the cumulative evidence (including the data presented in this paper) shows that the cold dust forms a separate component that is widely distributed within galaxies and contains at least an order of magnitude more mass than the warm (IRAS detected) dust.

Although a bolometric correction for cold dust emission was suggested by Disney et al. (1989), a physically extended dust component was first suggested by Valentijn (1990) to explain the results of a surface-brightness/inclination test that found galaxies did not change their surface-brightness with inclination. Also, Beckman et al. (1996) found strong color gradients in galaxies which, if due to dust, required a dust scale height larger than the stars. The conclusions drawn from these studies were not unique however; Davies et al. (1993) argued that Valentijn's surface-brightness/inclination test was invalid because of surface-brightness selection effects, and de Jong (1996) argued that the strong color gradients found by Beckman et al. were the result of differences in star formation history.

The first direct evidence (though still lacking confirmation) for an extended dust distribution came from Zaritski (1994). He measured the reddening of background galaxies seen in projection both close to and far away from two foreground galaxies. He claimed a detection of measurable reddening of the background galaxy population at a projected distance of 60 kpc from the foreground galaxy. The exponential scale length of the dust distribution was estimated to be about 30 kpc, consistent, for example, with the size of halos determined from QSO absorption line studies (Ostriker & Heisler 1984). This was a highly radical conclusion, the uncertainties in our understanding of the standard (IRAS) interstellar dust distribution (with a scale length of $\sim 3.5kpc$) was already leading to confusion in determinations of the optical opacity of spiral disks (Trewhella et al. 1997). To add another dust component would complicate the process still further.

We began the study of dust distribution as part of our ongoing initiative to understand the extinction in disk galaxies. We required more accurate dust distribution information as input to our radiative transfer models. In our first attempt to determine the distribution of dust more accurately (particularly the cold dust), we used the 140 and 240μm all-sky maps from the COBE satellite to constrain models of the far infrared emission from the Galaxy (Davies et al. 1997). Our results were surprising: we identified a diffuse, cold (18-22K) dust component with a scale height, ($\beta_d = 0.5kpc$) and scale length ($\alpha_d = 5.25$). These are longer than the stellar scale height ($\beta_s \approx 0.25$kpc) and stellar scale length ($\alpha_s \approx 3.5$kpc), and very different from the distribution of dust detected by IRAS, (which has $\beta_d = 0.5\beta_s$ and $\alpha_d \sim \alpha_s$ (Beichman 1987)). A cold dust component with these characteristics cannot be responsible for the prominent (optical) dust lanes seen in edge-on galaxies; these can only be produced by dust that is concentrated in the mid-plane. The COBE observations therefore suggest that the cold dust is a separate and more diffuse component than the warm dust seen by IRAS.

Our next line of evidence supporting the COBE result came from ISO. We mapped a sample of 10 nearby, resolved, late-type galaxies at 200μm using the C200 detector of ISOPHOT (Alton et al. 1998a). The radial scale lengths of the cold dust emission were significantly longer than those determined using observations at all the IRAS wavelengths. The emission was also stronger than expected by a simple extrapolation of the IRAS spectral energy distribution (SED), indicating the presence of a cold dust component that (a) contains $4-10\times$ the mass of the component detected by IRAS at the center and (b) becomes increasingly dominant in the outer regions.

The galaxy NGC 891, is often considered an ideal place to test ideas relating to dust opacity and distribution. It is the closest example of a highly inclined late-type spiral, allowing us to study dust above the galactic plane in detail. There have been 3 studies of this galaxy that lend further evidence to support the COBE and ISOPHOT results.

Xilouris et al. (1998) fitted a 3D radiative transfer model of stars and dust to optical and near infrared observations of NGC 891. They also found that the total dust mass was an order of magnitude larger than that detected by IRAS, and that the dust had a scale length in the radial direction that was larger than the stars. Howk and Savage (1997) took BVR images of NGC 891 in exceptional seeing (0.6") using the WIYN-3.5m telescope. The multicolor, high-resolution image highlights dust above the disk up to 1.5 *kpc* from the mid-plane. Recently, our SCUBA images of NGC 891 (Alton et al. 1998b) at $450\mu m$ and $850\mu m$ detected dust up to 2kpc from the mid-plane, confirmed the order of magnitude increase in dust mass over IRAS, observations, and showed that cold dust increasingly dominates the far infrared/submm spectrum at larger distances above the galactic plane.

We do have some concerns with regard to our interpretation of the above data. The COBE result depends upon a comparison of the observations with a rather idealized model. The ISOPHOT profiles are clearly more extended than those determined with IRAS but may be subject to detector memory effects. The Xilouris model is insensitive to diffuse dust that is distributed vertically with a longer scale length than the stars. The Howk and Savage observations only reveal areas where dust is more highly concentrated and does not predict any general flow from the disk. Our SCUBA observations do measure cold dust emission directly and have sufficient resolution to determine the dust extent above the disk. But, how general this phenomemon is remains to be seen; NGC 891 is an actively star forming galaxy and may not be representative of the general population.

For these reasons we have continued to obtain new observations which probe the dust distribution and temperature in different ways. In this paper we describe ISO Long Wavelength Spectrograph (LWS) observations of five galaxies (NGC 660, NGC 5194, NGC 5236, NGC 6946 and NGC 7331). We have measured the far infrared SED at two positions in each galactic disk: one at the galactic center and one some distance from the center. We can then compare the SEDs and look for the signature of cold dust at larger radii. The observations are described in section 2, our results are presented in section 3, we discuss our results in section 4 and state our overall conclusions in section 5.

2. Observations

The target galaxies were drawn from our sample of 10 nearby resolved galaxies mapped at $200\mu m$ with the ISOPHOT instrument on ISO (Alton et al. 1998a). All the galaxies in the sample have angular sizes greater than 8 arcmin. To obtain independent samples (considering the predicted LWS beam size was 99 arcsec) the pointings chosen were: the galaxy center (P1), a point 100 arcsec from the center (P2), and another at 200 arcsec from the center (P3). IRAS HiRes maps of the target galaxies at $100\mu m$ were used to assess the feasibility of each observation and pointings were discarded if the IRAS $100\mu m$ flux was less than $3.5Jy$ per beam. For the 3 largest galaxies (NGC 5194, NGC 5236 and NGC 6946) all three points were feasible; 2 points only were possible for the next largest galaxies (NGC 134, NGC 1448, NGC 4736 and NGC 7331); for the galaxies NGC 628 and NGC 660 only the center was bright enough and so these galaxies can only be used as a comparison with the central regions of the other galaxies. The allocated observing time allowed for observations of P1 and P3 of NGC 5194, NGC 5236 and NGC 6946; P1 and P2 of NGC 7331; and P1 of NGC 660. The aperture sizes and positions on each galaxy are shown overlaid onto an optical image in Figure 1.

The observations consisted of grating spectra over the full wavelength range ($43–197\mu m$) of the LWS instrument. The spectrum falls on ten separate detectors each of which overlaps in wavelength with its spectral neighbor and is independently calibrated. The integration times were calculated to give a S/N of 10 or greater at $100\mu m$ in a $0.6\mu m$ resolution element. The observations were performed between May 1, 1997 and August 23, 1997.

The data was initially processed with Pipeline 7.0, and then with the LWS interactive analysis program (LIA-v7). Within LIA, checks and re-evaluation (if deemed necessary) of the dark current, detector responsivity drift and calibration flashes were performed. The data was then re-processed to give the final spectra. ISAPv1.5 was used to search the data interactively for cosmic ray events (glitches) and their after effects. These were removed manually. The data from individual scans were averaged, and the ISAP de-fringing algorithm applied. LWS data reduction is described in detail in the LWS instrument data users manual.

3. Results

The derived spectral energy distributions at each position are shown in Figures 2-6. We have smoothed each spectrum with a Gaussian of FWHM $= 5\mu m$ (the original sampling was at $0.3 - 0.6\mu m$, depending on the detector) and displayed the data in flux density units (Jy) against wavelength (μm). The strong emission line at $\approx 158\mu m$ is due to CII. The spectrum from each detector is treated independently during the processing, and so the relative offsets between detectors give some crude indication of the reliability of the calibration and dark current subtraction. The agreement is reasonable (within 10%), although there are a few obvious exceptions to this. Generally, the flux from the 5 short wavelength detectors is untrustworthy when observing the faint, outer regions (due to the errors from the dark current subtraction being larger than the incident flux). We discuss below, the results for each galaxy.

3.1. NGC 660

NGC 660 is a nearby polar ring galaxy, with concentrated far infrared emission associated with a nuclear starburst (Alton et al. 1998a). The nuclear starburst gives this galaxy a high FIR/optical light ratio. It is likely to have the warmest central dust component and therefore provides an interesting comparison to the other, more quiescent galaxies. The LWS observations (Figure 2) show a SED that rises steeply from the mid-infrared to peak at around $100\mu m$ before falling off again into the far infrared.

3.2. NGC 5194

The far infrared SED of the almost face-on "Whirlpool Galaxy", M51, NGC 5194, is shown in Figure 3. As seen for NGC 660, the spectrum of the central regions (P1) rises steeply from the mid-infrared until it turns over at $\approx 100\mu m$; although it does not appear to drop-off beyond $100\mu m$ quite as rapidly as NGC 660. The P3 aperture lies in an inter-arm region some 6.2 kpc or 2.2 optical (B band) scale lengths from the galactic center. The SED of the outer regions (P3) is regrettably too noisy to be of use in this study.

3.3. NGC 5236

This well known, nearby, barred spiral almost certainly contains a mild nuclear starburst. As such, it might be expected that this galaxy would show a strong difference between the nuclear and outer disk SEDs. Indeed, the nuclear (P1) SED (Figure 4) appears remarkably similar to that of the starbursting NGC 660. The P3 aperture is some 6.9 kpc or 1.6 optical scale lengths from the galactic center and appears to straddle a spiral arm. The P3 SED rises steeply through the far infrared towards the sub-mm with no observed peak and is demonstrably different from the P1 spectrum.

3.4. NGC 6946

This almost face-on Sc galaxy also contains a mild nuclear starburst. The SED (Figure 5) at the P1 position is very similar to the other starburst regions (centers of NGC 660 and NGC 5236). The P3 aperture is 10.1 *kpc* or 1.4 optical scale lengths from the galactic center, devoid of very much optical emission, and apparently falling between spiral arms. Again, the outer P3 position appears to be dominated by longer wavelength emission, but even more dramatically than in the other galaxies. The spectrum is still steeply rising to the long wavelength limit of LWS.

3.5. NGC 7331

For NGC 7331 there was a problem with the positioning of the apertures and they are slightly off-set from those originally desired (Figure 1). Positions P1 and P2 were observed (not P3 as it was too faint) and so the outer aperture is not as far from the galactic center as in the other galaxies. But because this galaxy is inclined, the aperture does sample dust above the galactic plane. For these reasons, we might expect a less significant difference between the inner and outer regions. Still, P2 is 5.5 *kpc* or 2.2 optical scale lengths from the center and Figure 6 shows that the spectrum of NGC 7331 displays a marked difference between the central regions and outer disk, and may be compared with the observations of NGC 5194.

3.6. Comparison with IRAS and ISOPHOT

Given our objective, which was to confirm or reject our assertion that cold dust emission dominates at large distance from the galactic center, the absolute calibration of the spectra is not crucial: the important issue is how the relative SEDs change with position.

Even so, we have checked the calibration against previous observations of NGC 6946 made by IRAS and ISOPHOT. We have made simple beam-size corrections assuming a point source (center) and constant point spread function shape (outer regions). We have included the data points in Figure 5. The LWS calibrated data agree reasonably well to those measured by IRAS and ISOPHOT and show similar overall trends.

A very crude scale length (from 2 points) can be determined from the LWS spectra (assuming an exponential distribution). For NGC 6946, we find scale lengths of 60″, 70″ and 150″ at 60, 100 and 200μm respectively. These compare well with the scale lengths measured from full profiles, using the IRAS and ISOPHOT data, which were 87″, 82″ and 158″ for the 60, 100 and 200μm data respectively (Alton et al. 1998a).

Considering the observations were made with different telescopes, instruments, observing procedures and data reduction techniques and are subject to a rather uncertain beam correction, the agreement in both the flux values and the scale lengths is reasonable and adds confidence to our scientific results.

4. Discussion

The presence of an extended distribution of cold dust, that was entirely missed by IRAS, was suggested from controversial interpretations of indirect evidence (Valentijn 1990, Beckman et al. 1996). The first direct (but still controversial) observational evidence of its existence (Zaritsky 1994) has been slow to be accepted. Early criticisms and questions were: How could the dust get there? Or, was the result a statistical fluctuation? Certainly, modelling with only one warm component of dust is relatively easy and opposition to further complications is only natural. But, the gap between model and observations has steadily grown.

The LWS data presented in this paper clearly demonstrates that there is a distinct change in the SED with galactocentric radius in disk galaxies. The central regions of these galaxies are dominated by a warm component ($T \approx 30-35$K). The outer regions have spectra dominated by dust that has a SED peak beyond $200\mu m$ and so must be colder than $T \approx 20K$. This highlights the misleading impression that one can obtain from single-aperture far-infrared measurements of galaxies, which will always be dominated by the small, warm dust component at the center. Given the poor resolution of IRAS and ISO, the majority of detected galaxies will have very inaccurately determined dust temperatures and masses.

To illustrate this point we have assumed an exponential far infrared surface-brightness distribution and used the aperture photometry and approximate scale lengths calculated in section 3.6 to estimate the global fluxes of NGC 6946 at 60, 100 and $200\mu m$. These are normalized to the $60\mu m$ flux and compared to similar ratios at the center. The center regions give (60:100:200) 1 : 2.4 : 1.8 while the global values are 1 : 3.3 : 11.2.

To demonstrate how this spectral change could affect our understanding of the derived mass and temperature of the dust, we have fitted a two-component grey-body model ($\beta = 1.0$ and $\beta = 2.0$) to these relative spectra. The temperatures and mass ratios of the components are given in Table 1. The model spectra are shown in Figure 7, the units have been chosen so that the height of the graph is roughly proportional to the amount of energy a given wavelength contributes. For the central regions, the fits require a cold dust component with $2 - 14\times$ the mass of the warm component. These are consistent with our ISOPHOT results that found a central cold dust component containing $4 - 10\times$ the mass of the warm dust. The global fits have markedly different spectra. The fits for $\beta = 1.0$ and $\beta = 2.0$ both require cold dust components with temperatures of $T_C \approx 10K$; energy peaks at wavelengths of $300 - 400\mu m$; and $M_C \approx 700\times$ the mass of the warm dust component.

Although the above provides one possible fit to the LWS spectra, we should emphasize (as can be seen from Figure 7) that the cold dust component fits are poorly constrained due to the lack of data at wavelengths beyond $200\mu m$, and although we present the best (least squares) fit here, a large range of formal fits are allowable within the observational errors. The formal cold-dust temperature range is $2 < T_C < 25$ and M_C could vary by up to a factor of 100.

With the addition of the LWS results presented in this paper, there are now three pieces of observational evidence (Davies et al. 1997, Alton et al. 1998a) that the cold dust in galaxies is more spatially extended in the radial direction than the warm dust detected by IRAS. There are also now three pieces of observational evidence that suggest dust can be distributed to large distances above the plane of galaxy disks (Zaritsky 1994, Davies et al. 1997, Alton et al. 1998b).

In addition to the observational evidence, we now also have a better understanding of how dust might populate these outer regions. Greenberg (1987) considered the transport of dust into the halo showing that radiation pressure can expel dust to relatively large distances ($\approx 15kpc$) above the galactic plane. In nearby, edge-on galaxies, this dust injection can be seen around and above the star formation regions in the disk (Howk & Savage 1997, Ferrara 1996). We have recently investigated this further (Davies et al. 1998) and find that the expulsion distance is very dependent on the disk opacity: where optically thin disks can expel dust at high velocity to large distances. A significant dust enrichment of the halo therefore may well have occurred very early on in the life of a galaxy before the disk obtained a significant opacity. In present-day galaxies, this enrichment may only occur in proximity to star formation regions where the radiation pressure is exceptionally high.

With a theoretical framework of the mechanisms by which dust may populate halos of disk galaxies (and mounting observational evidence for its existence) it seems we cannot escape the conclusion that galaxies contain two components of dust: a spatially extended distribution of cold dust, and a concentrated warm dust component in the disk which is probably associated with star formation.

A second distinct component of dust obviously complicates the process of determining the extinction and opacity of spiral disks and a large halo of dust may significantly increase the obscuration of the distant Universe (Wright 1990, Fall & Pei 1993). It is also clear that our understanding of the star formation history and/or the dust mass budget of disks (Eales & Edmunds 1996) will have to be re-evaluated; the halo is being chemically enriched somehow, either through *in situ* star formation, or through transportation of material from star formation sites in the plane.

But, perhaps the most important implication of this result is the suggestion that the far infrared emission could be associated with cold dense halo clouds that could make up a significant fraction of the halo mass (Gerhard & Silk 1996). The cold dust itself cannot possibly account for the total halo mass, but if it were linked to the dominant mass compenent, the emission we detect could act as a tracer of the halo mass. Certainly, other molecular material has been tentatively detected in the outer parts of the Milky Way (Lequeux et al. 1993). Very recently H_2 has been discovered in enough quantity to account for all the missing mass in NGC 891 (Valentijn and van der Werf 1999). Molecular hydrogen is often linked with dust as it is believed that dust provides the major mechanism for converting neutral Hydrogen into H_2.

5. Conclusions

From analysis of our LWS observations of 5 disk galaxies our conclusions are:

1. The central SED is very similar to that inferred globally for galaxies by IRAS. The central SED peaks at $\sim 100\mu m$ leading to inferred dust temperatures of 30-35 K.

2. The SED in the outskirts of these galaxies is still rising at the last data point ($197\mu m$), indicating cold dust temperatures of less than 20 K.

3. Although a global measurement of the SED distribution (for example, a measurement of a distant galaxy subtending an angle smaller than the telescope point spread function) would indicate dust temperatures of 30-35K. In fact, there is probably at least an order of magnitude more cold dust than warm dust in galaxies.

4. There is increasing evidence, from a number of quite different sources, that the cold dust component is extensive around galaxies. This cold dust may be associated with the halos responsible for flat rotation curves.

We are extremely grateful to Sergio Molinari for his help with the data reduction and the use of the LWS interactive analysis software. We would also like to thank Rhodri Evans, Steve Lord and George Helou for their early comments and discussion of the results.

REFERENCES

Alton, P.B., Trewhella, M., Davies, J.I., Evans, Rh., Bianchi, S., Gear, W., Thronson, H., Valentijn, E., & Witt, A. 1998a, A&A, 335, 807

Alton, P.B., Bianchi, S., Rand, R.J., Xilouris, E.M., Davies, J.I., & Trewhella, M. 1998b, ApJ, 507, L129

Beckman, J., Peletier, R., Knapen, J., Corradi, R. & Gentet, L., 1996 ApJ, 467, 175

Beichman, C. 1987, ARA&A, 25, 521

Bianchi, S., Ferrara, A., & Giovanardi, C. 1996, ApJ, 465, 127

Bianchi, S., Ph.D. Thesis, University of Wales

Davies, J., Phillipps, S., Boyce, P., & Disney M. 1993, MNRAS, 260, 491

Davies, J.I., Trewhella, M., Jones, H., Madden, A., Moss, J. & Lisk, C. 1997, MNRAS, 28, 679

Davies, J.I., Alton, P., Bianchi, S. & Trewhella, M. 1998, MNRAS, 300, 1006

Devereux, N. & Young, J. 1990, ApJ, 359, 42

Disney, M., Davies, J.I. & Phillipps, S. 1989, MNRAS, 239, 939

Eales, S., & Edmunds, M.G. 1996, MNRAS, 280, 1167

Fall, S.M., & Pei, Y.C. 1993, ApJ, 402, 479

Ferrara, A. 1996, in The Physics of Galactic Halos, ed. Lesch H., Springer-Verlag, Berlin

Gerhard, O. & Silk, J. 1996, ApJ, 472, 34

Greenberg, M., Ferrini, F., Barsells, B., & Aiello, S. 1987, Nature, 327, 214

Hiltner, W., & Johnson H., 1956, ApJ, 124, 367

Howk, J., & Savage, B. 1997, AJ,114, 2463

de Jong, R. 1996, A&A, 313, 377

Kylafis, N., & Bahcall, J. 1987, ApJ, 317, 637

Lequeux, J., Allen, R., & Guilloteau, S. 1993, A&A, 280, L23

Ostriker, J.P., & Heisler, J., 1984, ApJ, 287, 1

Trewhella, M., Davies J.I., Disney, M., & Jones,H. 1997, MNRAS, 288, 397

Trewhella, M., Madore, B.F., & Kuchinski, L. 1999, ApJ, in preparation

Valentijn, E. 1990, Nature, 346, 153.

Witt, A.N., Thronson, H.A., & Capuano, J.M. 1992, ApJ, 393, 611

Wright, E. 1990, ApJ, 353, 411

Xilouris, E.M, Alton, P.B., Davies, J.I., Kylafis, N., Papamastorakis, J., & Trewhella, M. 1998, A&A, 331, 894

Zaritsky, D. 1994, AJ, 108, 1619

This manuscript was prepared with the AAS LaTeX macros v4.0.

Fig. 1.— LWS pointings for galaxy sample. The observed effective apertures for each galaxy are shown overlaid on optical (from DSS) and $100\mu m$ (IRAS HiRes) images.

Fig. 2.— Spectral energy distribution of NGC 660 in the central regions.

Fig. 3.— Spectral energy distribution of NGC 5194. The upper panel shows the central regions, the lower panel shows a point $200''$ from the center. The detectors where the signal is less than the errors in the dark current subtraction (SW1, SW2, SW3 and SW4) have been omitted from the plot.

Fig. 4.— Spectral energy distribution of NGC 5236. The upper panel shows the central regions, the lower panel shows a point $200''$ from the center. The detectors where the signal is less than the errors in the dark current subtraction (SW1, SW2, SW3 and SW4) have been omitted from the plot.

Fig. 5.— Spectral energy distribution of NGC 6946. The upper panel shows the central regions, the lower panel shows a point $200''$ from the center. The detectors where the signal is less than the errors in the dark current subtraction (SW1, SW2, SW3 and SW4) have been omitted from the plot.

Fig. 6.— Spectral energy distribution of NGC 7331. The upper panel shows the central regions, the lower panel shows a point $100''$ from the center.

Fig. 7.— Comparison of the global SED of NGC 6946 with the SED at the center. The central fluxes are well fit by a 2 component model with $2 - 14\times$ the mass in the cold component as in the warm. For the global fits however, the outer regions require a cold dust component with a mass $\approx 700\times$ that of the warm dust component.

Table 1. Central and Global 2 Component Fits to NGC 6946 Data

		$\beta = 1.0$			$\beta = 2.0$	
Position	T1	T2	N2/N1	T1	T2	N2/N1
Center	32.5	22.0	1.9	32.0	19.0	14
Global	30.0	9.5	708	26.0	9.5	747

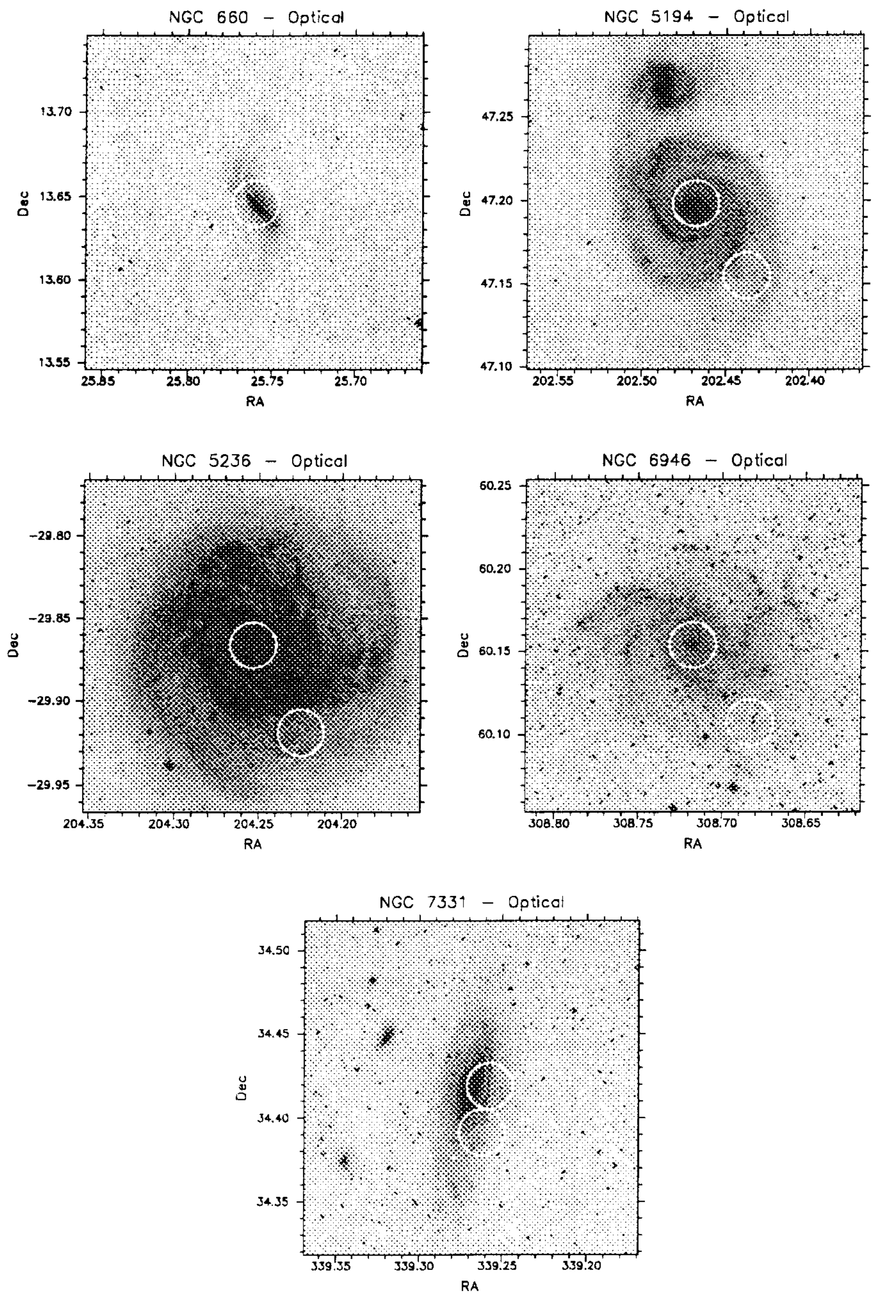
NGC 660 – Optical
13.70
13.65
13.60
13.55
Dec
25.85
25.80
25.75
25.70
RA
NGC 5194 – Optical
47.25
47.20
47.15
47.10
Dec
202.55
202.50
202.45
202.40
RA
NGC 5236 – Optical
−29.80
−29.85
−29.90
−29.95
Dec
204.35
204.30
204.25
204.20
RA
NGC 6946 – Optical
60.25
60.20
60.15
60.10
Dec
308.80
308.75
308.70
308.65
RA
NGC 7331 – Optical
34.50
34.45
34.40
34.35
Dec
339.35
339.30
339.25
339.20
RA

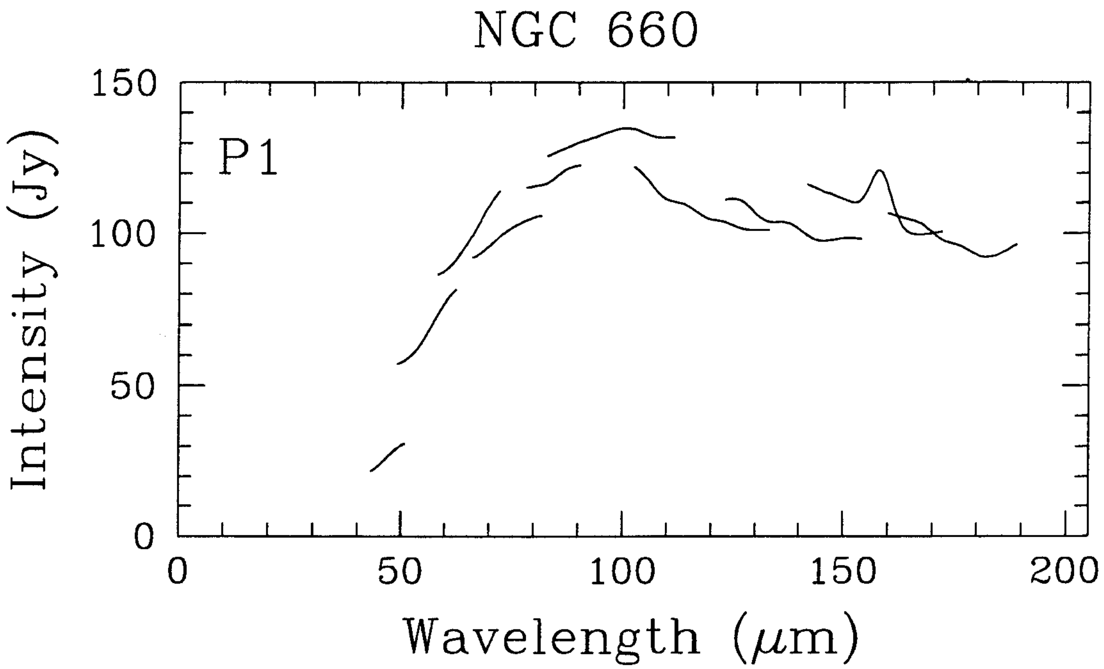
NGC 660
P1
Intensity (Jy)
Wavelength (μm)
0
50
100
150
200

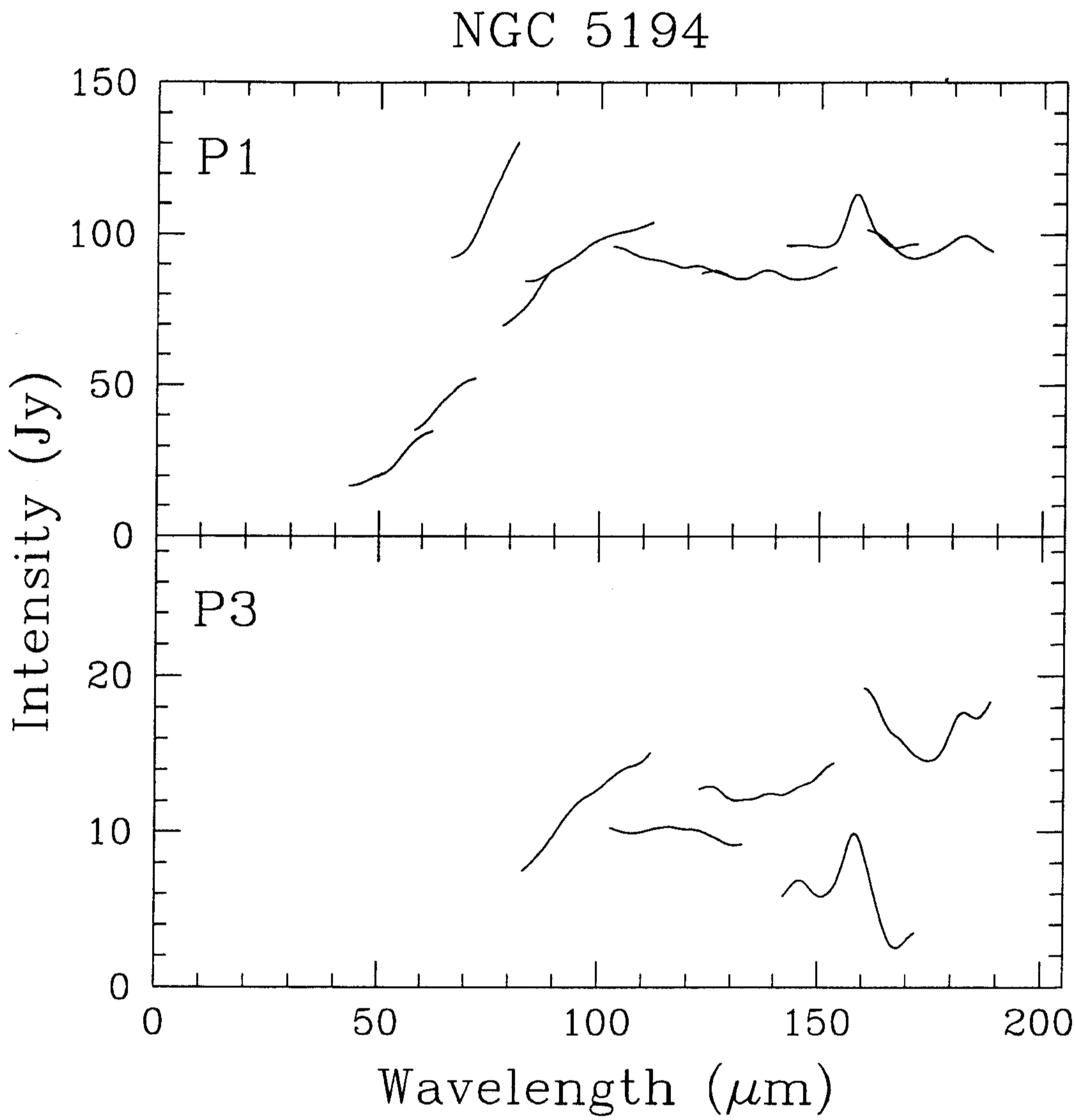
NGC 5194
P1
P3
Intensity (Jy)
Wavelength (μm)
0
50
100
150
0
10
20
0
50
100
150
200

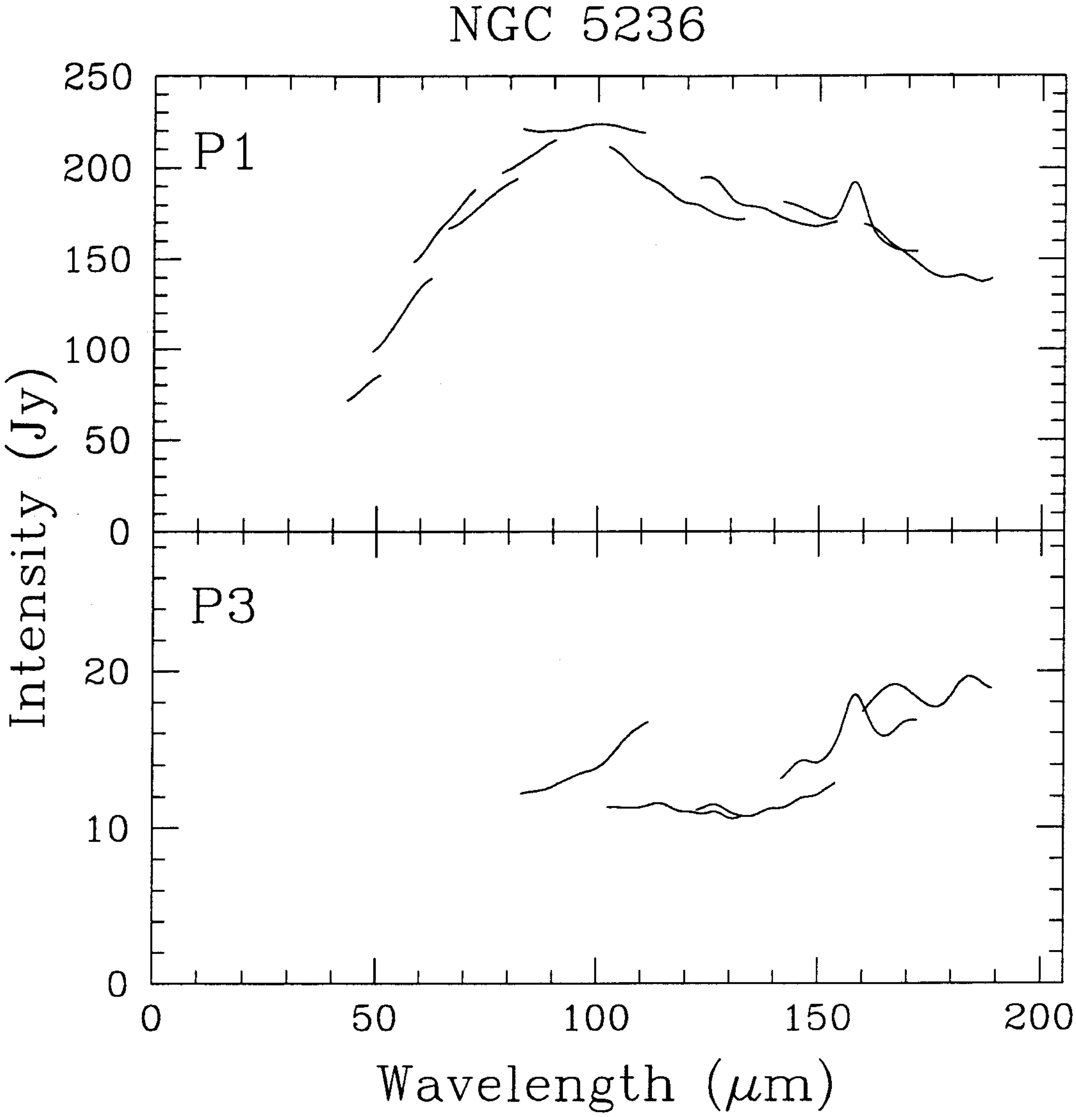
NGC 5236
P1
P3
Intensity (Jy)
Wavelength (μm)
250
200
150
100
50
0
20
10
0
0
50
100
150
200

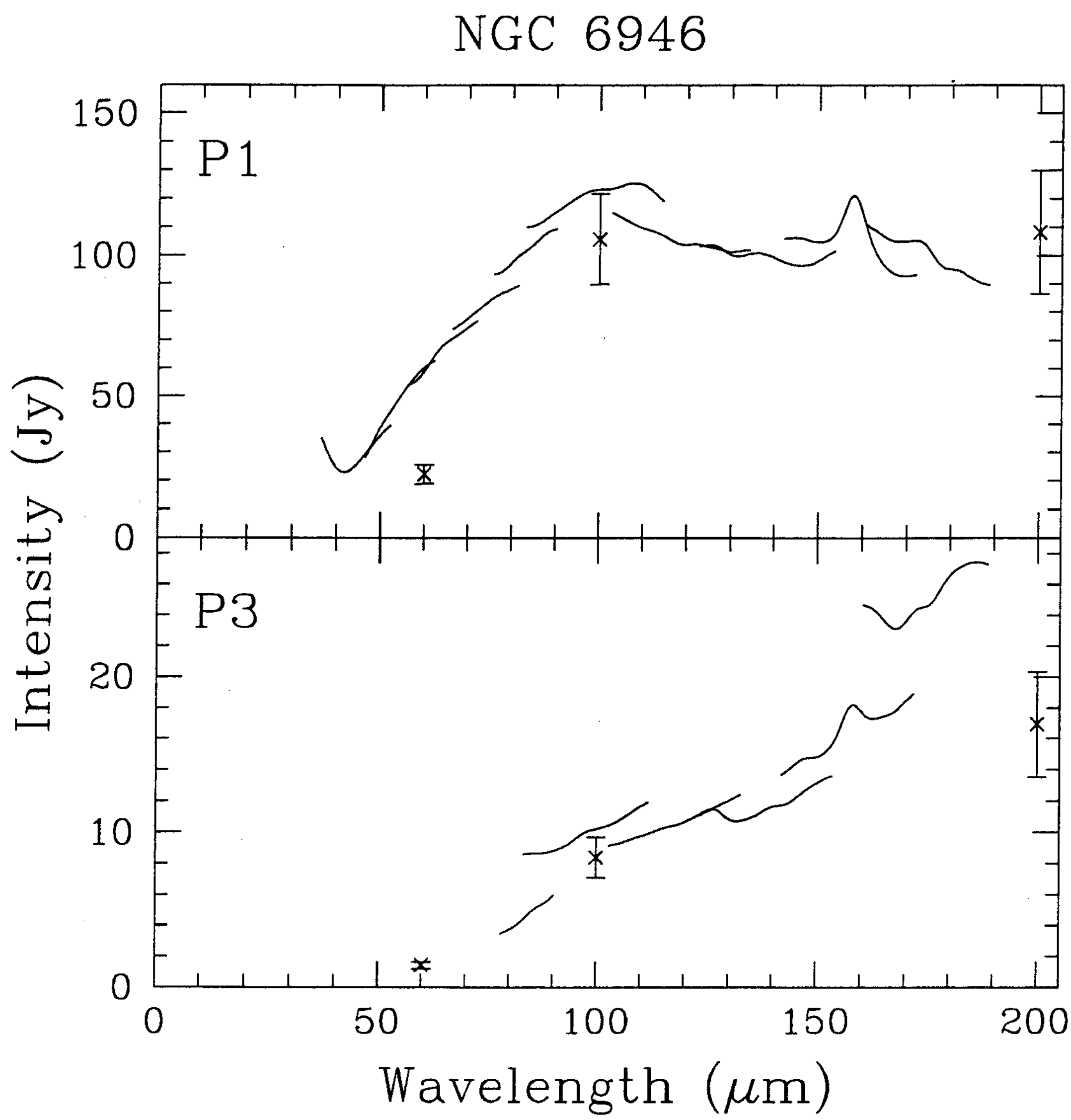
NGC 6946
P1
P3
Intensity (Jy)
Wavelength (μm)
0
50
100
150
0
10
20
0
50
100
150
200

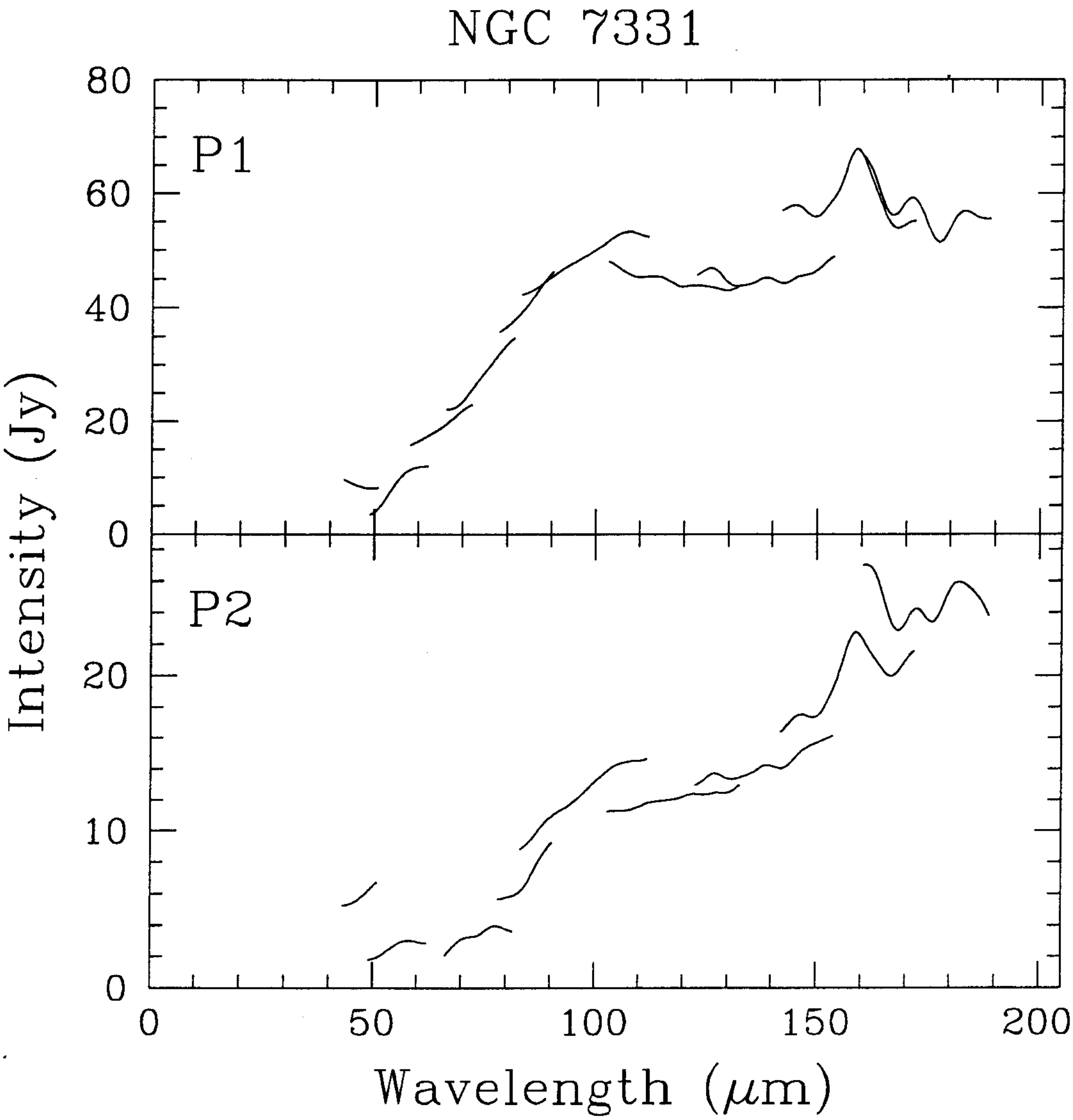
NGC 7331
P1
P2
Intensity (Jy)
Wavelength (μm)
0
20
40
60
80
10
50
100
150
200

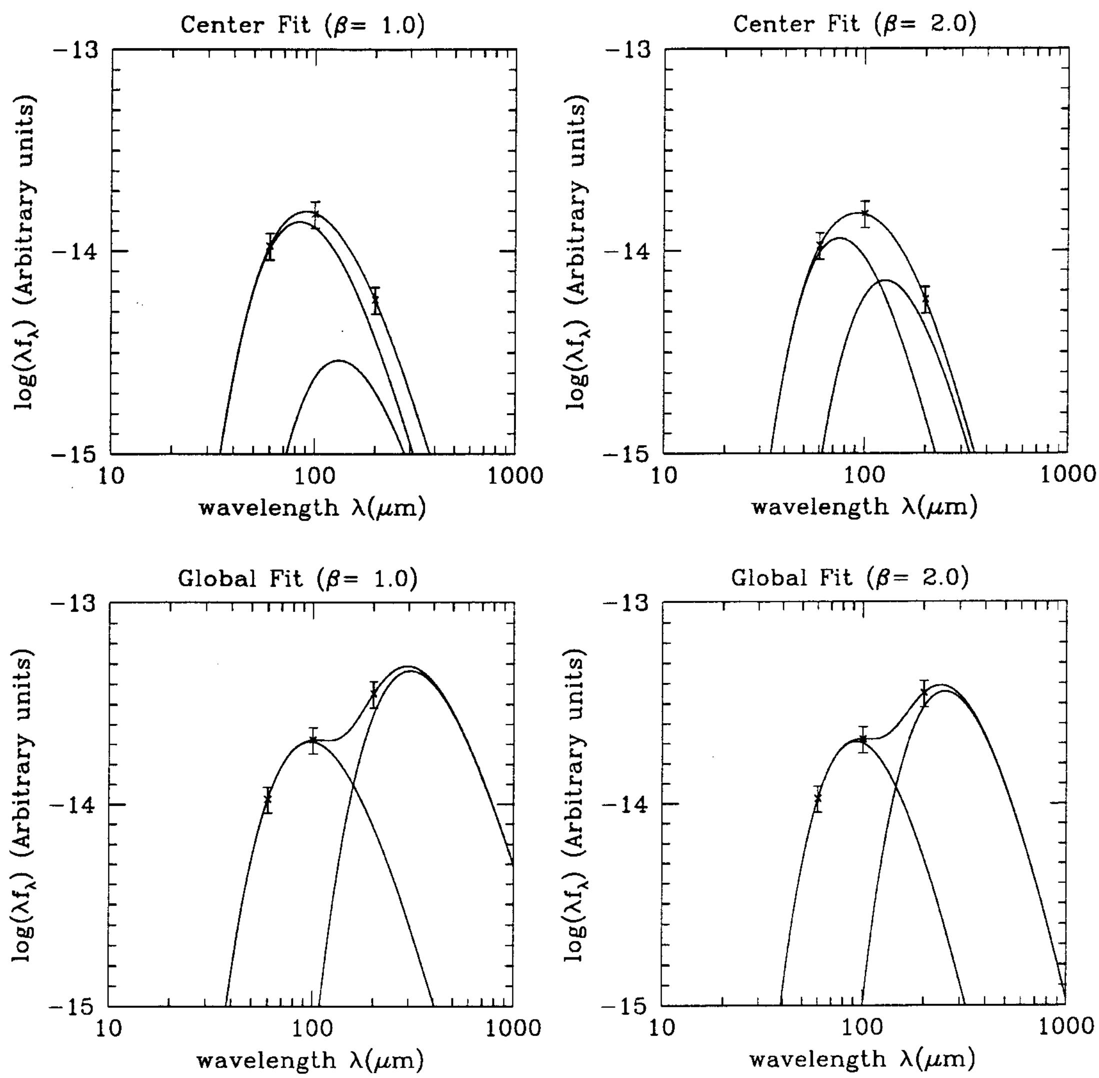
Center Fit (β= 1.0)
Center Fit (β= 2.0)
Global Fit (β= 1.0)
Global Fit (β= 2.0)
log(λf_λ) (Arbitrary units)
wavelength λ(μm)
−13
−14
−15
10
100
1000